Variable-frequency-controlled coupling in charge qubit circuits: Effects of microwave field on qubit-state readout

Xiao-Ling He,[1,2] Yu-xi Liu,[3,2] J. Q. You,[1,2] and Franco Nori[2,3,4]

[1]*Department of Physics and Surface Physics Laboratory (National Key Laboratory), Fudan University, Shanghai 200433, China*

[2]*Frontier Research System, The Institute of Physical and Chemical Research (RIKEN), Wako-shi 351-0198, Japan*

[3]*CREST, Japan Science and Technology Agency (JST), Kawaguchi, Saitama 332-0012, Japan*

[4]*Center for Theoretical Physics, Physics Department, Center for the Study of Complex Systems, The University of Michigan, Ann Arbor, Michigan 48109-1040, USA*

(Received 22 March 2007; published 17 August 2007)

To implement quantum-information processing, microwave fields are often used to manipulate superconducting qubits. We study how the coupling between superconducting charge qubits can be controlled by variable-frequency magnetic fields. We also study the effects of the microwave fields on the readout of the charge-qubit states. The measurement of the charge-qubit states can be used to demonstrate the statistical properties of photons.

DOI: 10.1103/PhysRevA.76.022317 PACS number(s): 03.67.Lx, 85.25.Cp

I. INTRODUCTION

Superconducting quantum circuits are good candidates for implementing quantum-information processing [1,2]. To construct universal quantum computing, controllable couplings between any pair of qubits are required. Theoretical methods for switchable couplings in charge-qubit circuits have been proposed by changing the amplitude of the bias magnetic flux, e.g., in Refs. [2–4]. However, in experiments, it is much easier to produce precise *frequency* shifts of the radio-frequency (rf) control signals, as opposed to changing the *amplitude* of the dc signal. Methods using variable-frequency-controlled couplings in superconducting flux-qubit circuits have been studied [5] theoretically, comparing with the coupling approach using the dressed states [6–8]. In this scheme, the two qubits can be coupled to (or decoupled from) each other by modulating the frequencies [5] of externally applied variable-frequency magnetic fields to match (or mismatch) the combination of frequencies of the two qubits. The coherent oscillations and conditional gate operations of two superconducting charge qubits with always-on coupling have been demonstrated [9] experimentally. Therefore the next step for charge qubits would be to design superconducting quantum circuits with switchable couplings.

Here, we first generalize our approach [5] using the variable-frequency-controlled coupling in *flux* qubit circuits to the *charge* qubit circuit proposed in Ref. [4]. This proposal has the following advantages: (i) the coupling between different charge qubits can be implemented by changing the frequency of the externally applied classical field; (ii) these proposed charge qubits always work at their optimal points, and thus the qubits are mostly immune from charge noise [10], produced by uncontrollable charge fluctuations; (iii) no additional circuit is needed to realize this controllable coupling.

Besides the controllable coupling, measuring the qubit state is also a very important step in quantum information processing. In superconducting quantum circuits, microwave fields are often used to implement quantum rotations. Here we focus on how microwave fields affect the readouts of the qubit states. In particular, we explore the effect of quantized fields with different statistical properties on measurement results of the qubit states when the charge qubits are placed inside a microcavity, e.g., a three-dimensional cavity [11,12] or a superconducting transmission line [13].

The paper is organized as follows: In Sec. II, we generalize the variable-frequency-controlled coupling approach in flux-qubit circuits [5] to that in charge-qubit circuits [4]. In Sec. III, we study the effect of the classical and quantized microwave fields on the readout of the qubit states. In Sec. IV, we compare the classical and quantum treatment of the large Josephson junction. Finally, conclusions are presented in Sec. V.

II. HAMILTONIAN WITH VARIABLE-FREQUENCY CONTROLLED COUPLINGS

We first very briefly review the model Hamiltonian proposed in Ref. [4] for two coupled superconducting charge qubits by sharing a large Josephson junction (JJ) (see Fig. 1). The large JJ is classically treated and its charging energy E_{c0} is neglected. The dc biased magnetic field Φ_e is externally applied through the area between the large JJ and the first qubit. Each qubit is also biased by a dc voltage V_{Xi} via the gate capacitance C_i $(i=1,2)$. The Hamiltonian of the superconducting circuit is [4]

$$H=\sum_{i=1}^{2}\left[E_i(V_{Xi})-2E_{Ji}\cos\left(\frac{\pi\Phi_e}{\Phi_0}-\frac{\gamma}{2}\right)\cos\varphi_i\right]-E_{J0}\cos\gamma \tag{1}$$

with $E_i(V_{Xi})=E_{ci}(n_i-C_iV_{Xi}/2e)^2$. Here $E_{ci}=2e^2/(C_i+2C_{Ji})$ and E_{Ji} are the charge and Josephson energies of the ith charge qubit. E_{J0} is the Josephson energy of the large JJ. The number n_i of excess Cooper pairs in the superconducting island is canonically conjugate to the average phase drop $\varphi_i=(\varphi_{iA}+\varphi_{iB})/2$ of the ith charge qubit. The phase drop across the large JJ is γ. Considering that the critical current $I_0\equiv 2\pi E_{J0}/\Phi_0$ of the large JJ is much larger than the critical

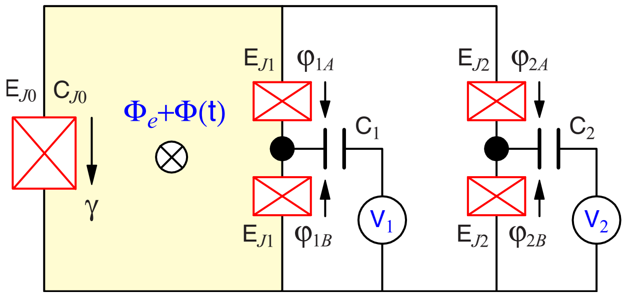

FIG. 1. (Color online) Schematic diagram of two charge qubits coupled by a (left) large Josephson junction (JJ) with coupling energy E_{J0} and capacitance C_{J0}. For the ith charge qubit (where $i=1,2$), a superconducting island (denoted by a filled circle) is connected to two identical small JJs (each with coupling energy E_{Ji} and capacitance C_{Ji}). Also, this island is biased by the voltage $V_i=V_{Xi}+V_g^{(i)}(t)$ via a gate capacitance C_i, where V_{Xi} is a static (dc) gate voltage and $V_g^{(i)}(t)$ is a time-dependent (ac) microwave gate voltage. Moreover, a static (dc) magnetic flux Φ_e plus a microwave-field-induced magnetic flux $\Phi(t)$ (ac) are applied to the (yellow) region between the large JJ and the first charge qubit.

currents $I_{ci}\equiv 2\pi E_{Ji}/\Phi_0$ of the charge qubits, the phase γ across the large JJ is very small. We can expand the functions of the phase drop γ in Eq. (1) into a series and retain the terms up to second order in the parameters $\eta_i=(I_{ci}/I_0)<1$. In this case, Eq. (1) can be reduced to

$$H=\sum_{i=1}^{2}[\varepsilon_i(V_{Xi})\sigma_z^{(i)}-\bar{E}_{Ji}\sigma_x^{(i)}]-\chi_{12}\sigma_x^{(1)}\sigma_x^{(2)} \tag{2}$$

in the spin-$\frac{1}{2}$ representation based on the charge states $|0\rangle\equiv|\uparrow\rangle$ and $|1\rangle\equiv|\downarrow\rangle$ that correspond to zero and one excess Cooper pair in each Cooper-pair box, where $\varepsilon_i(V_{Xi})=\frac{1}{2}E_{ci}(C_iV_{Xi}/e-1)$, and

$$\bar{E}_{Ji}=E_{Ji}\cos\left(\frac{\pi\Phi_e}{\Phi_0}\right)\left[1-\frac{3}{8}\sin^2\left(\frac{\pi\Phi_e}{\Phi_0}\right)(\eta_i^2+3\eta_j^2)\right],$$

with $i,j=1,2$ $(i\neq j)$. The coupling strength χ_{12} between the two charge qubits is

$$\chi_{12}=L_JI_{c1}I_{c2}\sin^2\left(\frac{\pi\Phi_e}{\Phi_0}\right), \tag{3}$$

where $L_J=\Phi_0/2\pi I_0$ is the Josephson inductance of the large JJ. It is clear that the coupling between the two qubits is realized via this effective inductance.

Now, we study how to apply our variable-frequency-controlled approach [5] to the above charge-qubit circuits [4]. We assume that besides the dc voltages V_{Xi} and the dc magnetic flux Φ_e, an ac microwave voltage $V_g^{(i)}(t)=V_{gi}\cos(\omega_{gi}t)$ with the frequency ω_{gi} is applied to the superconduction island of the ith qubit via its gate capacitance, and an additional variable-frequency (ac) magnetic flux $\Phi(t)=\Phi_c\sin(\omega t)$ is also applied through the area between the large JJ and the first charge qubit (see Fig. 1). To make our proposed charge-qubit more immune from the uncontrollable charge fluctuations, it is also assumed that two charge qubits work at their optimal points, i.e., the applied dc voltages V_{Xi} satisfy the condition $\varepsilon_i(V_{Xi})=0$. Considering these conditions, the Hamiltonian in Eq. (2) becomes

$$H=\sum_{i=1}^{2}[-\bar{E}_{Ji}\sigma_x^{(i)}+\varepsilon_0^{(i)}\cos(\omega_{gi}t)\sigma_z^{(i)}]-\chi_{12}\sigma_x^{(1)}\sigma_x^{(2)}$$
$$+[g_{12}\sigma_x^{(1)}\sigma_x^{(2)}-\sum_{i=1}^{2}(g_i\sigma_x^{(i)})]\sin(\omega t), \tag{4}$$

where $\varepsilon_0^{(i)}=E_{ci}(C_iV_{gi}/2e)$ and $g_i=2E_{Ji}\sin(\pi\Phi_e/\Phi_0)\xi$. The parameters g_{12} and ξ are given by

$$g_{12}=L_JI_{c1}I_{c2}\sin\left(\frac{2\pi\Phi_e}{\Phi_0}\right)J_1(\varphi_c),$$

and

$$\xi=J_1(\varphi_c)\left\{1-\frac{3(\eta_i^2+3\eta_j^2)}{16}\left[1-\cos\left(\frac{2\pi\Phi_e}{\Phi_0}\right)J_0(\varphi_c)\right]\right\}$$
$$+\frac{3}{8}\cos^2\left(\frac{\pi\Phi_e}{\Phi_0}\right)J_0(\varphi_c)J_1(\varphi_c)(\eta_i^2+3\eta_j^2).$$

Here $\varphi_c=2\pi\Phi_c/\Phi_0$ and J_n is the nth-order Bessel function of the first kind.

In the rotating reference frame at the frequency ω_{gi} about $\sigma_x^{(i)}$, the Hamiltonian in Eq. (4) is rewritten as

$$H=\sum_{i=1}^{2}[(\hbar\omega_{gi}-\bar{E}_{Ji})\sigma_x^{(i)}+\varepsilon_0^{(i)}\sigma_z^{(i)}]-\chi_{12}\sigma_x^{(1)}\sigma_x^{(2)}$$
$$+\left(g_{12}\sigma_x^{(1)}\sigma_x^{(2)}-\sum_{i=1}^{2}g_i\sigma_x^{(i)}\right)\sin(\omega t). \tag{5}$$

To eliminate the $\sigma_x^{(i)}$ term in Eq. (5), the frequency ω_{gi} of the microwave field applied to the gate capacitance is set as $\hbar\omega_{gi}\simeq\bar{E}_{Ji}$. Furthermore, we can tune the flux Φ_e so that the coupling strength χ_{12} is less than the coupling strength g_{12}. Also, we tune the gate voltage V_{gi} so that the large detuning condition $|\varepsilon_0^{(2)}-\varepsilon_0^{(1)}|=\Delta\gg\chi_{12}$ can be satisfied. Under this condition, the always-on interaction χ_{12} is negligibly small, and the Hamiltonian in Eq. (5) is reduced [14] to

$$H\approx\sum_{i=1}^{2}\hbar\omega_i\sigma_z^{(i)}+\left(g_{12}\sigma_x^{(1)}\sigma_x^{(2)}-\sum_{i=1}^{2}g_i\sigma_x^{(i)}\right)\sin(\omega t), \tag{6}$$

with $\hbar\omega_1=\varepsilon_0^{(1)}-\chi'$, $\hbar\omega_2=\varepsilon_0^{(2)}+\chi'$, and $\chi'=\chi_{12}^2/2\Delta$.

Let us discuss how the interaction between two qubits can be switched on and off via Eq. (6) by changing the frequency ω of the variable-frequency magnetic flux $\Phi(t)=\Phi_c\sin(\omega t)$. Equation (6) shows that the two qubits are approximately decoupled from each other when there is no applied ac magnetic flux $\Phi(t)$. However, if the frequency ω of $\Phi(t)$ is tuned to satisfy the condition $\omega=\omega_1+\omega_2$, then two qubits can be simultaneously flipped by the variable-frequency magnetic flux via the interaction Hamiltonian

$$V_I = g_{12}\sigma_-^{(1)}\sigma_-^{(2)} + g_{12}^*\sigma_+^{(1)}\sigma_+^{(2)}, \tag{7}$$

where the contributions of other fast oscillating terms are negligibly small. If the frequency ω of $\Phi(t)$ satisfies the condition $\omega=\omega_2-\omega_1$, then one qubit can be flipped by another with the help of the variable-frequency magnetic flux through the interaction Hamiltonian

$$V_I' = g_{12}\sigma_+^{(1)}\sigma_-^{(2)} + g_{12}^*\sigma_-^{(1)}\sigma_+^{(2)}, \tag{8}$$

after neglecting other fast oscillating terms.

A single-qubit operation can also be implemented via the variable-frequency magnetic flux $\Phi(t)$. For example, if $\omega=\omega_1$, or $\omega=\omega_2$, then the first or second qubit can be selectively rotated around the x axis. When there is no variable-frequency magnetic flux, a rotation around the z axis can be implemented for each qubit. Therefore any logic gate (see, e.g., Ref. [15]) can be realized by using single-qubit operations and two-qubit operation via the Hamiltonians in Eqs. (7) and (8).

III. EFFECT OF MICROWAVE FIELDS ON SUPERCURRENTS IN THE MEASUREMENT OF QUBIT STATES

Above, we have shown that the interaction between the two qubits can be switched on and off using a variable-frequency magnetic flux. Two-qubit operations can be implemented, and entangled states between two qubits can also be generated, using Eqs. (7) or (8). To implement the readout of two-qubit states, we need to calculate the circulating supercurrent $\hat{I}$ contributed by the two qubits [4]. The operator of the supercurrent $\hat{I}$ of the two qubits is given by

$$\hat{I} = \sin\left(\frac{\pi\Phi_e}{\Phi_0}\right)(I_{c1}\sigma_x^{(1)} + I_{c2}\sigma_x^{(2)}) - \frac{1}{4I_0}\sin\left(\frac{2\pi\Phi_e}{\Phi_0}\right) \times (I_{c1}^2 + I_{c2}^2 + 2I_{c1}I_{c2}\sigma_x^{(1)}\sigma_x^{(2)}). \tag{9}$$

For any given state (e.g., $|\Psi\rangle$) of two qubits, the supercurrent can be obtained by

$$I = \langle\Psi|\hat{I}|\Psi\rangle. \tag{10}$$

Note that two-qubit operations are always related to the microwave fields. The supercurrent I might be different for different microwave fields with different statistical properties. Below, we study how the different microwave fields affect the supercurrent I.

A. Classical microwave field

We now focus on two-qubit entangled states, created from the ground state $|g_1,g_2\rangle$ via the two-qubit interaction Hamiltonian in Eq. (7). For these created entangled two-qubit states, the contribution of the average values of single-qubit operators $\sigma_x^{(i)}$ $(i=1,2)$ to the supercurrent is zero, and the supercurrent I is only determined by the two-qubit operator $\sigma_x^{(1)}\sigma_x^{(2)}$ as follows:

$$\langle\hat{I}\rangle = -\frac{\eta I_c}{2}\sin\left(\frac{2\pi\Phi_e}{\Phi_0}\right)(1+\langle\sigma_x^{(1)}\sigma_x^{(2)}\rangle). \tag{11}$$

Here, for simplicity, the two qubits are supposed to have identical critical supercurrent $I_{c1}=I_{c2}=I_c$, and then $\eta_1=\eta_2=\eta$. The quantum fluctuation of the total supercurrent $\hat{I}$ is

$$\overline{(\Delta\hat{I})^2} = \langle\hat{I}^2\rangle - \langle\hat{I}\rangle^2, \tag{12}$$

which can be further given by

$$\overline{(\Delta\hat{I})^2} = \frac{\eta^2}{4}I_c^2\sin^2\left(\frac{2\pi\Phi_e}{\Phi_0}\right)[1-(\langle\sigma_x^{(1)}\sigma_x^{(2)}\rangle)^2] + 2I_c^2\sin^2\left(\frac{\pi\Phi_e}{\Phi_0}\right)(1+\langle\sigma_x^{(1)}\sigma_x^{(2)}\rangle). \tag{13}$$

Considering that the ratio η is small, the first term in Eq. (13) can be neglected in the following calculations. In this case, the supercurrent fluctuation has a similar behavior to the supercurrent $\langle\hat{I}\rangle$ of Eq. (11) and $\overline{(\Delta\hat{I})^2}\propto\langle\hat{I}\rangle$, when entangled two-qubit states are created from the ground state $|g_1,g_2\rangle$ through the Hamiltonian in Eq. (7). For convenience, we define a reduced quantity κ to describe the supercurrent $\langle\hat{I}\rangle$ and supercurrent fluctuation $\overline{(\Delta\hat{I})^2}$ as

$$\kappa(\tau) = 1+\langle\sigma_x^{(1)}\sigma_x^{(2)}\rangle = \frac{\overline{(\Delta\hat{I})^2}}{2I_c^2\sin^2(\pi\Phi_e/\Phi_0)} = \frac{-2\langle\hat{I}\rangle}{\eta I_c\sin(2\pi\Phi_e/\Phi_0)}. \tag{14}$$

If two charge qubits are initially in an entangled state $(\cos\theta)|g_1,g_2\rangle+(\sin\theta)e^{i\phi}|e_1,e_2\rangle$ and the evolution of the two qubits is governed by the Hamiltonian in Eq. (7), then the reduced supercurrent or supercurrent fluctuation $\kappa(\tau)$ can be given by

$$\kappa_c = 1+\sin(2\theta)\cos(\tau)\cos\phi+\cos(2\theta)\sin(\tau), \tag{15}$$

which means that κ_c is an ac signal. Here, $\tau=|g_{12}|t$, with the evolution time t. If the initial state is $(\cos\theta)|g_1,g_2\rangle+(\sin\theta)|e_1,e_2\rangle$, then $\kappa_c=1+\sin(\tau+2\theta)$. When the evolution time $\tau_0=-2\theta+2n\pi-\frac{\pi}{2}$, $\kappa_c=0$, which gives rise to $\langle\sigma_x^{(1)}\sigma_x^{(2)}\rangle=-1$. Thus in this case both the total supercurrent and the supercurrent fluctuation become zero.

B. Quantized microwave field

Now let us consider the case when the variable-frequency magnetic flux $\Phi_c\cos(\omega t)$ is replaced by a quantized magnetic flux, $\Phi_q a^+ + \Phi_q^* a$, with frequency $\omega=\omega_1+\omega_2$. Following the same way as the above derivation of Eq. (7), we can obtain an interaction Hamiltonian H_I between the quantized magnetic flux and the two charge qubits,

$$H_I = \xi_{12}a^+\sigma_-^{(1)}\sigma_-^{(2)} + \xi_{12}^* a\sigma_+^{(1)}\sigma_+^{(2)}, \tag{16}$$

where

$$\xi_{12} = -\frac{2\pi\Phi_q L_J I_{c1} I_{c2}}{\Phi_0}\sin\left(\frac{2\pi\Phi_e}{\Phi_0}\right). \tag{17}$$

This model indicates that one photon can flip both qubits simultaneously.

We now consider that the two qubits are initially in the state $(\cos\theta)|g,g\rangle + (\sin\theta)e^{i\phi}|e,e\rangle$ and the quantum field is initially in a state $\Sigma D(n)|n\rangle$, here $D(n)$ will be given below for a given state. From the Hamiltonian (16), the total system evolves to

$$\Psi(\tau) = \sum_{n=0}^{n=\infty}[a_n(\tau)|e,e,n\rangle + b_n(\tau)|g,g,n+1\rangle] + (\cos\theta)D(0)|g,g,0\rangle, \tag{18}$$

where

$$a_n(\tau) = \cos(\tau\sqrt{n+1})(\sin\theta)e^{i\phi}D(n) - \sin(\tau\sqrt{n+1})(\cos\theta)D(n+1),$$

$$b_n(\tau) = \cos(\tau\sqrt{n+1})(\cos\theta)D(n+1) + \sin(\tau\sqrt{n+1})(\sin\theta)e^{i\phi}D(n),$$

with the rescaled dimensionless time $\tau = |\xi_{12}|t$. Using Eqs. (14) and (18), at the time τ, the reduced supercurrent expectation value or supercurrent fluctuation $\kappa_q(\tau)$ in the case of the quantized field is

$$\kappa_q(\tau) = 1 + 2\,\mathrm{Re}\left(w_0(\tau)(\cos\theta)D(0) + \sum_{n=0}^{\infty}[u_n(\tau)v_n(\tau)]\right), \tag{19}$$

where

$$w_0(\tau) = (\cos\tau)(\sin\theta)e^{-i\phi}D^*(0) - (\sin\tau)(\cos\theta)D^*(1),$$

$$u_n(\tau) = \cos(\tau\sqrt{n+2})(\sin\theta)e^{-i\phi}D^*(n+1) - \sin(\tau\sqrt{n+2})(\cos\theta)D^*(n+2),$$

$$v_n(\tau) = \cos(\tau\sqrt{n+1})(\cos\theta)D(n+1) + \sin(\tau\sqrt{n+1})(\sin\theta)e^{i\phi}D(n).$$

Equation (19) shows that the supercurrent expectation value $\langle\hat{I}\rangle$ consists of a dc component $-(\eta I_c/2)\sin(2\pi\Phi_e/\Phi_0)$ and different ac components, which are modulated by time-dependent factors, e.g., $\cos(\tau\sqrt{n+1})$.

We further specify that the quantized field is initially in several different quantum states [16], e.g., (i) the coherent state

$$|\alpha\rangle = e^{-\bar{n}/2}\sum\frac{\alpha^n}{\sqrt{n!}}|n\rangle, \tag{20}$$

with $\alpha = \sqrt{\bar{n}}e^{i\varphi}$; (ii) the superposition of two coherent states,

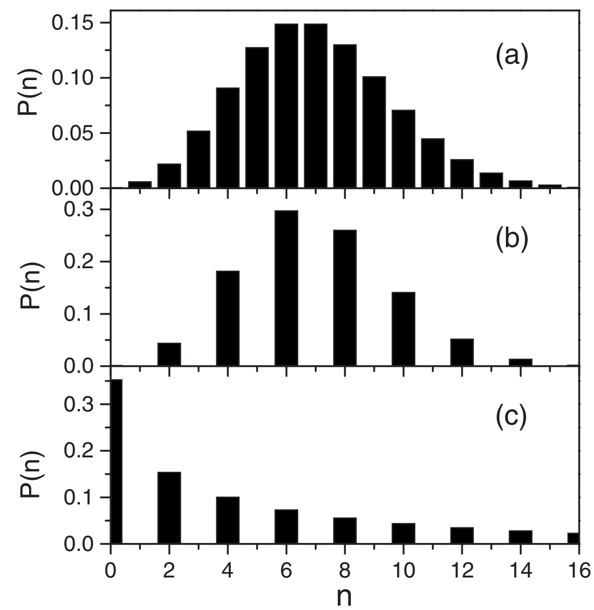

FIG. 2. The photon number distribution $P(n)$ with average photon number $\bar{n}=7$ of (a) coherent state $|\alpha\rangle$; (b) superposition of coherent states $(|\alpha\rangle + |-\alpha\rangle)/N_+$; and (c) squeezed vacuum state $|0,\zeta\rangle$.

$$|\alpha_s\rangle = \frac{1}{N_+}(|\alpha\rangle + |-\alpha\rangle) = \sum\frac{\alpha^{2n}}{\sqrt{(2n)!\cosh\bar{n}}}|2n\rangle, \tag{21}$$

with $N_+ = \sqrt{2(1+e^{-2\bar{n}})}$; and (iii) the squeezed vacuum state,

$$|0,\zeta\rangle = \sum\frac{\sqrt{(2n)!}}{n!\sqrt{\cosh r}}[-e^{i\beta}\tanh(r/2)]^n|2n\rangle, \tag{22}$$

with the squeezing parameter $\zeta \equiv re^{i\beta}$ and $\bar{n} = \sinh^2 r$. Here, $\bar{n}$ is the average photon number. The photon number distributions $P(n)$ [e.g., $P(n) = |D(n)|^2 = |\langle n|\alpha\rangle|^2$ for a coherent state] of the above three states are shown in Fig. 2. Physically, coherent states display Poissonian distribution, and the fluctuations of both quadrature components are equal to the standard quantum fluctuation limit, $\Delta X_1 = \Delta X_2 = 1/2$. Squeezed states have sub-Poisson distribution, and the fluctuation for one of the quadrature components can be squeezed, e.g., $\Delta X_1 < 1/2$.

If the qubits are initially in the ground state $|g_1,g_2\rangle$ and the quantized field is initially in the coherent state $|\alpha\rangle$, the reduced supercurrent expectation value or the supercurrent fluctuation is obtained from Eq. (19):

$$\kappa_q(\tau) = 1 - 2\cos\varphi e^{-\bar{n}}\sum_{n=0}^{\infty}A(n)\sin(\tau\sqrt{n+1})\cos(\tau\sqrt{n}), \tag{23}$$

with $A(n) = \bar{n}^{(n+1/2)}/(n!\sqrt{n+1})$. Equations (19) and (23) show that the supercurrent expectation value $\langle\hat{I}\rangle$ and the supercurrent fluctuation $\overline{(\Delta\hat{I})^2}$ are very sensitive to the phase φ of the coherent state. If $\varphi = \pi/2$, κ_q has only a dc component; however, when $\varphi \neq \pi/2$, κ_q consists of many different ac components.

If the qubits are initially in the ground state $|g_1,g_2\rangle$, but the quantized fields are initially in the squeezed vacuum states or superposition of coherent states, then from Eq. (19), $\kappa_q(\tau)$ is given by

$$\kappa_q(\tau) = 1 - 2\sum_{n=0}^{\infty} \mathrm{Re}[B(n)\sin(\tau\sqrt{n+1})\cos(\tau\sqrt{n})], \quad (24)$$

with $B(n)=D^*(n+1)D(n)$. Because of $D(2n+1)=0$, then $B(n)=0$ and $\kappa_q(\tau)=1$. Thus the oscillatory evolution disappears.

From Eq. (14), we know that the macroscopic supercurrent expectation value $\langle\hat{I}\rangle$ can be described by κ_q. Figure 3 shows that the supercurrent of the charge qubits are different with the same initial qubit state $(|g,g\rangle+|e,e\rangle)/\sqrt{2}$ but with different initial states of the quantum field. From Eq. (19), in the case of the coherent state $|\alpha\rangle$ with the phase $\varphi=\pi/2$, the total supercurrent $\langle\hat{I}\rangle$ displays a sinusoidal-like evolution, as shown in Fig. 3(a). However, when $\varphi=0$, the total supercurrent is shown in Fig. 3(b). If the quantized field is initially in a superposition of coherent states, the total supercurrent $\langle\hat{I}\rangle$, as shown in Fig. 3(c), demonstrates the collapse and partial-revival phenomena. In the case of the squeezed vacuum state, the total supercurrent approximately displays an ac current with a quasiperiodic evolution, which is demonstrated by Fig. 3(d). All irregular oscillations of the supercurrent expectation or supercurrent fluctuation reflect the coherent interference that comes from the coherent superpositions of the different photon number states. The different initial photon states result in different output of the measurement of the charge-qubit states. Therefore the measurement of the charge-qubit states can demonstrate the statistical properties of the photons, and charge qubits could serve as photon detectors.

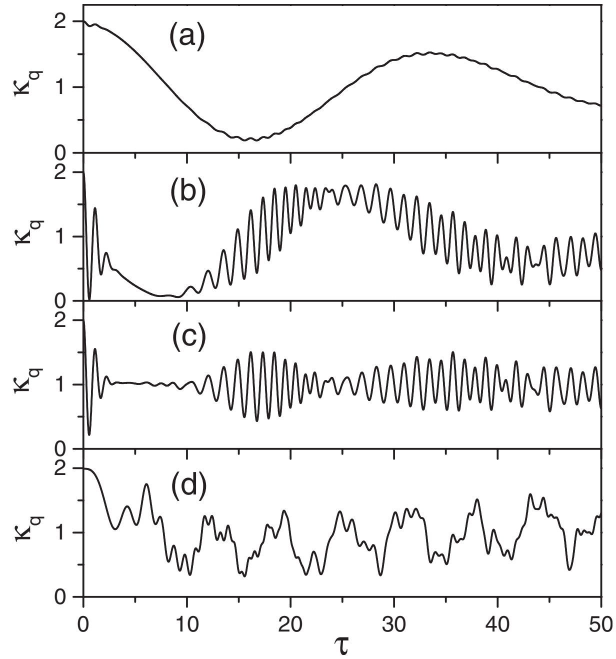

FIG. 3. Evolution $\kappa_q(\tau)$ of the reduced total supercurrent expectation and reduced supercurrent fluctuation from the initial qubit state $(|g,g\rangle+|e,e\rangle)/\sqrt{2}$ in the presence of the quantum field initially in (a) coherent state $|\alpha\rangle$ with the phase $\varphi=\pi/2$; (b) coherent state $\varphi=0$; (c) superposition of coherent states $(|\alpha\rangle+|-\alpha\rangle)/N_+$ with $\varphi=0$; (d) squeezed vacuum state $|0,\zeta\rangle$. The irregularity of oscillations originates from the interference effect of the photon component of the above states. Note that both $\kappa_q(\tau)$ and the rescaled time τ are dimensionless.

IV. QUANTIZATION TREATMENT ON LARGE JOSEPHSON JUNCTION

In the Hamiltonian (1), the charging energy term $E_{c0}N^2$ of the large JJ is neglected and the large JJ acts as an effective inductance L_J [4,17]. We now consider a quantum mechanical treatment for the large JJ. Considering the additional term of charging energy $E_{c0}N^2$, the Hamiltonian of the large JJ can be written as

$$H_0 = E_{c0}N^2 - E_{J0}\cos\gamma, \quad (25)$$

with the charging energy E_{c0} and the excess Cooper pairs N. Because the large JJ works in the phase regime, the spectrum of the large JJ is approximately equivalent to a harmonic oscillator $H_0=\hbar\omega_p a^\dagger a$, with the plasma frequency

$$\omega_p = \frac{1}{\hbar}\sqrt{8E_J^{(0)}E_c^{(0)}}. \quad (26)$$

The bosonic operators a and $a^\dagger$ are defined by

$$a = \frac{\varsigma}{2}\gamma + i\frac{1}{2\varsigma}N, \quad a^\dagger = \frac{\varsigma}{2}\gamma - i\frac{1}{2\varsigma}N, \quad (27)$$

and the phase drop γ is expressed as

$$\gamma = \frac{1}{\varsigma}(a^\dagger + a), \quad (28)$$

with $\varsigma=(E_J^{(0)}/2E_c^{(0)})^{1/4}$. Due to the large critical supercurrent of the large JJ, one can expand the phase drop γ in Eq. (1) into a series and retain terms to the first order of γ. Finally, a spin-boson interaction between the two charge qubits and the large JJ is achieved:

$$H = \sum_{i=1}^{2}\left[\varepsilon_i(V_{xi})\sigma_z^{(i)} - E_{Ji}\cos\left(\frac{\pi\Phi_e}{\Phi_0}\right)\sigma_x^{(i)}\right] + \hbar\omega_p a^\dagger a + \sum_{i=1}^{2}[g_{i0}\sigma_x^{(i)}(a^\dagger + a)], \quad (29)$$

where $g_{i0}=-(E_{Ji}/2\varsigma)\sin(\pi\Phi_e/\Phi_0)$. We assume that the plasma frequency ω_p of the large JJ is much larger than the splitting of the qubits. Thus the large JJ is always in the ground state when the qubits are operated. Following the standard technique of adiabatic elimination [14], we can eliminate the bosonic mode of the large JJ and obtain an effective interaction Hamiltonian between the two qubits: $\chi_{12}\sigma_x^{(1)}\sigma_x^{(2)}$, with the coupling strength $\chi_{12}=-2g_{10}g_{20}/\hbar\omega_p$. Using the expression of g_{10}, g_{20}, and ω_p, one can easily confirm that this interqubit coupling is the same as that in Eq. (2). Here the large JJ serves as the data bus to virtually mediate the interaction between the two qubits. Therefore the classical and quantum treatment to the large JJ are equivalent to each other. Generalizing the two-qubit system to the multiqubit system, the effective interqubit coupling term reads $\Sigma_{i>j}\chi_{ij}\sigma_x^{(i)}\sigma_x^{(j)}$ with $\chi_{ij}=-2g_{i0}g_{j0}/\hbar\omega_p$. Because $g_{i0}=-(E_{Ji}/2\varsigma)\sin(\pi\Phi_e/\Phi_0)$, the coupling χ_{ij} is tunable by changing the static magnetic field Φ_e applied to the loop. We should point out that if the dc magnetic flux Φ_e is replaced by an ac variable-frequency magnetic flux $\Phi_e(t)$, then the qubit can be selectively coupled to the data bus by a well-chosen frequency-matching condition between the qubit, data bus, and the variable-frequency magnetic flux.

V. CONCLUSIONS

In summary, we have studied a variable-frequency-control approach in charge-qubit circuits: the switchable coupling between the two charge qubits can be implemented by changing the frequency of the externally applied magnetic flux. Single-qubit operations can also be addressed and operated selectively. The charge qubits are chosen to work at their optimal points, so the effect of the noise, resulting from uncontrollable charge fluctuations, on the charge qubits is much suppressed. Moreover, the effects of the microwave field on the supercurrent of the two qubits are discussed. It is found that the supercurrent of the qubits significantly depends on the states of the microwave field. We also discuss the quantum treatment of the large JJ and find that both quantum and classical treatments are equivalent to each other. If the two-qubit circuit is generalized to many qubits, the interaction $\sigma_x^{(i)}\sigma_x^{(j)}$ can also be achieved.

ACKNOWLEDGMENTS

F.N. was supported in part by the US National Security Agency (NSA), Army Research Office (ARO), Laboratory of Physical Sciences (LPS), and National Science Foundation Grant No. EIA-0130383. X.L.H. and J.Q.Y. were supported by PCSIRT, SRFDP, and NFRPC Grant No. 2006CB921205, and the National Natural Science Foundation of China Grants No. 10534060 and No. 10625416.

[1] J. Q. You and F. Nori, Phys. Today **58** (11), 42 (2005).
[2] Y. Makhlin, G. Schön, and A. Shnirman, Rev. Mod. Phys. **73**, 357 (2001).
[3] J. Q. You, J. S. Tsai, and F. Nori, Phys. Rev. Lett. **89**, 197902 (2002); A longer version of it is available in e-print arXiv:cond-mat/0306203; see also *New Directions in Mesoscopic Physics*, edited by R. Fazio, V. F. Gantmakher, and Y. Imry (Kluwer Academic, New York, 2003), p. 351.
[4] J. Q. You, J. S. Tsai, and F. Nori, Phys. Rev. B **68**, 024510 (2003).
[5] Y. X. Liu, L. F. Wei, J. S. Tsai, and F. Nori, Phys. Rev. Lett. **96**, 067003 (2006).
[6] C. Rigetti, A. Blais, and M. Devoret, Phys. Rev. Lett. **94**, 240502 (2005).
[7] Y. X. Liu, C. P. Sun, and F. Nori, Phys. Rev. A **74**, 052321 (2006).
[8] S. Ashhab, S. Matsuo, N. Hatakenaka, and F. Nori, Phys. Rev. B **74**, 184504 (2006).
[9] Yu. A. Pashkin, T. Yamamoto, O. Astafiev, Y. Nakamura, D. V. Averin, and J. S. Tsai, Nature (London) **421**, 823 (2003); T. Yamamoto, Yu. A. Pashkin, O. Astafiev, Y. Nakamura, D. V. Averin, and J. S. Tsai, *ibid.* **425**, 941 (2003).
[10] D. Vion, A. Aassime, A. Cottet, P. Joyez, H. Pothier, C. Urbina, D. Esteve, and M. H. Devoret, Science **296**, 886 (2002).
[11] J. Q. You and F. Nori, Phys. Rev. B **68**, 064509 (2003).
[12] Y. X. Liu, L. F. Wei, and F. Nori, Europhys. Lett. **67**, 941 (2004); Y. X. Liu, L. F. Wei, and F. Nori, Phys. Rev. A **71**, 063820 (2005).
[13] A. Blais, R. S. Huang, A. Wallraff, S. M. Girvin, and R. J. Schoelkopf, Phys. Rev. A **69**, 062320 (2004).
[14] Y. X. Liu, L. F. Wei, and F. Nori, Phys. Rev. A **72**, 033818 (2005).
[15] D. Deutsch, A. Barenco, and A. Ekert, Proc. R. Soc. London, Ser. A **449**, 669 (1995).
[16] M. Orszag, *Quantum Optics* (Springer, Berlin, 2000).
[17] M. Grajcar, A. Izmalkov, S. H. W. van der Ploeg, S. Linzen, E. Il'ichev, Th. Wagner, U. Hubner, H.-G. Meyer, Alec Maassen van den Brink, S. Uchaikin, and A M. Zagoskin, Phys. Rev. B **72**, 020503(R) (2005).